

## A New "123" Family: $LnBa_2Fe_3O_z$

I.  $Ln = Dy, Ho$

E. GARCÍA-GONZÁLEZ\*·§ M. PARRAS,\*  
J. M. GONZÁLEZ-CALBET,\*·†·¶ AND M. VALLET-REGÍ†·‡

\*Departamento de Química Inorgánica, Facultad de Químicas, Universidad Complutense, 28040-Madrid, Spain; †Instituto de Magnetismo Aplicado, RENFE-UCM, Apdo. Correos 155, 28230-Las Rozas (Madrid), Spain; and ‡Departamento de Química Inorgánica y Bioinorgánica, Facultad de Farmacia, Universidad Complutense, 28040-Madrid, Spain

Received July 22, 1992; accepted October 7, 1992

The microstructural characterization of  $LnBa_2Fe_3O_8$  materials ( $Ln = Dy, Ho$ ) has been carried out by means of electron diffraction and high resolution electron microscopy. The results obtained lead to a lattice with tetragonal symmetry and parameters  $a_c \times a_c \times 3a_c$  ( $a_c$  being the perovskite subcell parameter) and  $P4/mmm$  as possible space group. A structural model in which two square pyramids [ $FeO_5$ ] and one octahedron [ $FeO_6$ ] alternate along the  $c$  axis is proposed. © 1993 Academic Press, Inc.

### Introduction

It is well known that the substitution of either  $A$  or  $B$  cations by other ions of lower oxidation state in  $ABO_3$  perovskites can lead to different phases of general composition  $ABO_{3-y}$ .

In the  $RE-Ba-Cu-O$  system ( $RE =$  Rare Earth), the different anionic coordinations that can be adopted by the copper [Cu(II)-Cu(III)] atoms (square, square pyramidal, and octahedral coordinations) have allowed several oxygen-deficient perovskites (1-3). Since the discovery of the  $YBa_2Cu_3O_7$  superconductor material (4), the 1:2:3,  $RE:Ba:B$  ( $B =$  transition metal) ratio has been the most widely studied. Complete replacement of Cu(1) and Cu(2) atoms (positions) by other cations with the same or a different type of coordination would give important

information about why copper seems to be necessary for superconductivity to occur.

Full substitution of Cu(1) and Cu(2) by Co has been achieved with simultaneous doping with K in the Ba positions (5). The resulting compound,  $Y(K_{0.5}Ba_{1.5})Co_3O_8$ , was found to have the basic  $YBa_2Cu_3O_{6+x}$  structure with two Co atoms in square pyramidal coordination and one Co atom octahedrally coordinated.

When iron is substituted by copper maintaining the cationic ratio 1:2:3, the differences in stability at the metallic sites lead to other results in the  $RE-Ba-Fe-O$  system.

Accordingly, we have carried out a study on the accommodation of compositional variations in  $LnBa_2Fe_3O_z$  ( $Ln = Nd, Sm, Eu, Gd, Dy$  and  $Ho$ ) (6), on which significant structural changes are observed depending on the lanthanide introduced. During the course of this work, both the nuclear and magnetic structures of  $YBa_2Fe_3O_8$  (7) have been reported; the configuration of the atoms in the unit cell is very similar to that of the superconductor  $YBa_2Cu_3O_7$ , with the

§ Work submitted in partial fulfillment of the degree of Doctor of Chemistry by E.G.G., Universidad Complutense, Madrid, April 1992.

¶ To whom correspondence should be addressed.

exception that the iron ions corresponding to the Cu-chain ions have octahedral coordination, rather than square planar. Due to this occupancy of the oxygen sites, the Ba ions show twelfold coordination, rather than tenfold.

We discuss, in this paper, the microstructural characterization of  $Dy(Ho)_{1/3}Ba_{2/3}FeO_{3-y}$  materials by means of electron diffraction (ED) and high resolution electron microscopy (HREM).

### Experimental

Samples of nominal composition  $Ln_{1/3}Ba_{2/3}FeO_{3-y}$  ( $Ln = Dy, Ho$ ) were prepared by heating stoichiometric mixtures of  $BaCO_3$ ,  $Ln_2O_3$ , and  $\alpha-Fe_2O_3$  of Anala R quality at  $1300^\circ C$  for 72 h. in air. The homogeneous black products were quenched at room temperature in the platinum crucibles used for synthesis.

The oxidation state of iron was determined by titration after dilution in 3 *N* HCl with an excess of Mohr salt.

Powder X-ray diffraction was performed on a D-5000 diffractometer with a graphite monochromator and using  $CuK\alpha$  radiation.

Electron diffraction was carried out on a JEOL 2000FX electron microscope, fitted with a double tilting goniometer stage ( $\pm 45^\circ$ ). High resolution electron microscopy was performed on a JEOL 4000EX electron microscope fitted with a double tilting goniometer stage ( $\pm 25^\circ$ ) by working at 400 Kv. Samples were ultrasonically dispersed in *n*-butanol and then transferred to carbon-coated copper grids.

### Results and Discussion

From the chemical analysis data it appears that all iron is found in the III oxidation state. Thus, the average composition of the samples is  $Dy(Ho)_{1/3}Ba_{2/3}FeO_{2.67}$ , i.e.,  $Dy(Ho)Ba_2Fe_3O_8$ .

X-ray diffraction patterns show the presence of two pseudocubic perovskite phases. The overall ratio of  $Ln:Ba:Fe$  in both

phases has been measured by EDX. The former, being related to the  $Ba_2Fe_2O_5$  oxide, has been discussed in a previous paper (8); the latter, being the most abundant and showing  $Dy(Ho)Ba_2Fe_3O_8$  composition, is what we present here.

Figures 1a, b, and c show a set of ED patterns corresponding to  $Dy(Ho)Ba_2Fe_3O_8$  along the  $[001]_c$ ,  $[0\bar{1}1]_c$ , and  $[1\bar{1}1]_c$  zone axes,<sup>1</sup> respectively. It is observed that all spots can be indexed on the basis of a cubic perovskite cell. However, the  $[010]_c$  projection (Fig. 2a) reveals the presence of superstructure spots tripling the  $c^*$  axis. By tilting around the  $[001]_c$  direction, the  $[1\bar{1}0]$  projection is obtained (Fig. 2b). The ensemble of the electron diffraction results lead to a reciprocal lattice analogous to the one corresponding to the  $YBa_2Cu_3O_{6+x}$  ( $0 < x < 1$ ) oxide, which is also a threefold superstructure of the cubic perovskite cell (9). The real lattice would present tetragonal symmetry, parameters  $a_c \times a_c \times 3a_c$ , and  $P4/mmm$  as possible space group.

In order to get qualitative structural information, individual crystals were aligned so that the electron beam was parallel to one of the main orientations of crystallographic interest. Thus, Figs. 3a and b show high resolution images along the  $[010]_c$  and  $[1\bar{1}0]_c$  zone axes, respectively, for  $Dy(Ho)Ba_2Fe_3O_8$ , a well ordered material with lattice fringe spacing equal to 1.18 nm ( $\approx 3 a_c$ ) along the  $c$  axis.

Taking into account both the occupancy of the A sublattice ( $Ba:Ln$  ratio) and the oxygen stoichiometry, two factors can be jointly or separately, the origin of the threefold superstructure:

- relative order of the  $Dy(Ho)$  and Ba atoms in the A sublattice, and
- anionic vacancies ordering.

From a crystallographic point of view, the presence of tetrahedral sites for iron in the  $AFeO_{3-y}$  ferrites implies the formation of

<sup>1</sup> Subindex  $_c$  refers to the basic perovskite cubic subcell.

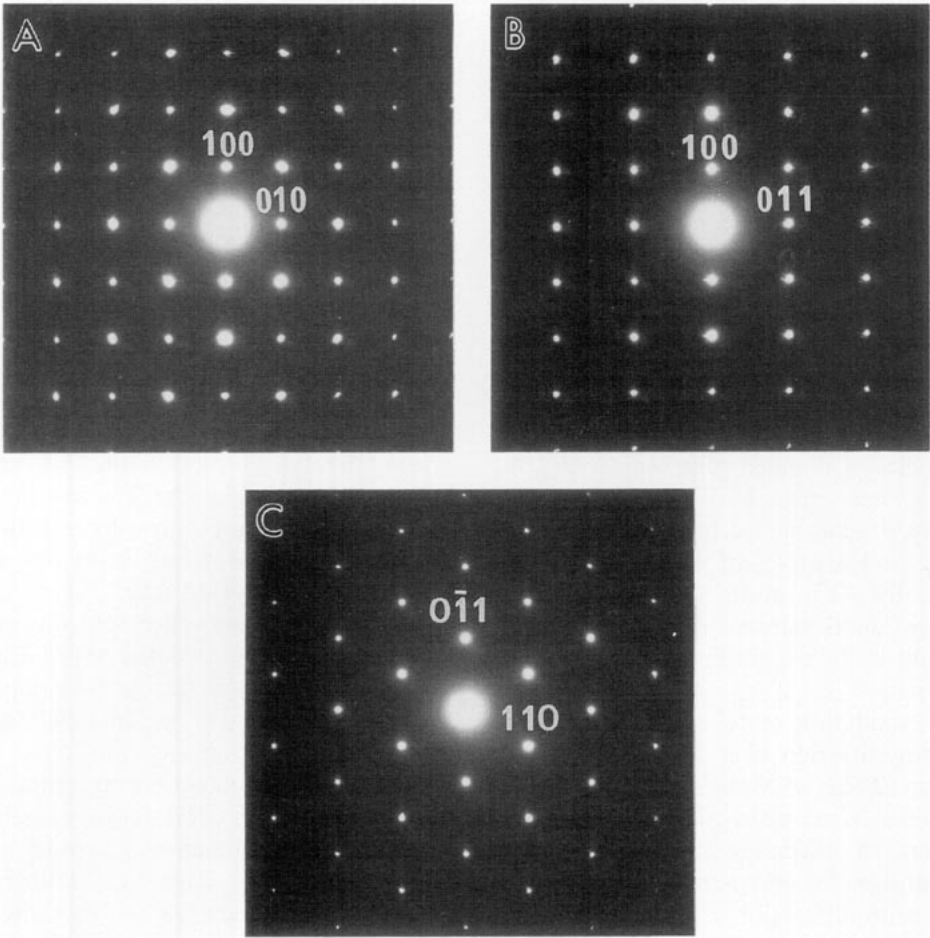


FIG. 1. Electron diffraction patterns corresponding to the  $\text{DyBa}_2\text{Fe}_3\text{O}_8$  material along the (a)  $[001]_c$ , (b)  $[011]_c$ , and (c)  $[111]_c$  zone axes.

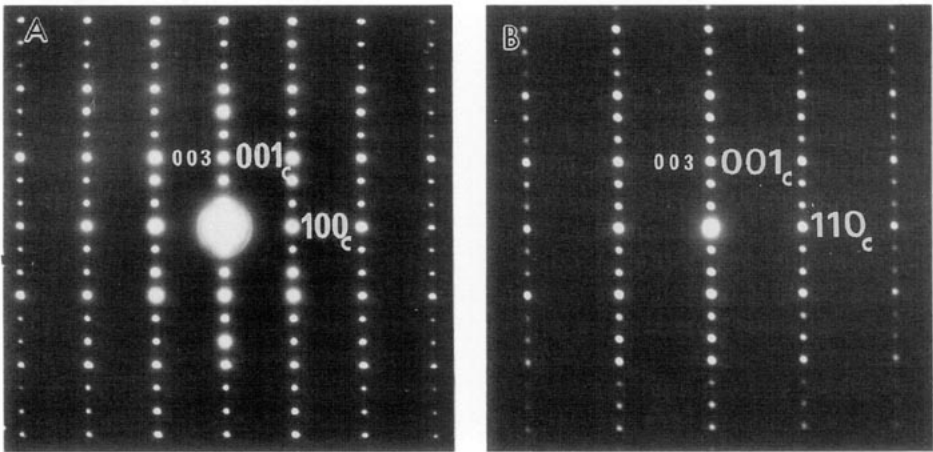


FIG. 2. Electron diffraction patterns for  $\text{DyBa}_2\text{Fe}_3\text{O}_8$  along the (a)  $[010]_c$  and (b)  $[\bar{1}\bar{1}0]_c$  zone axes.

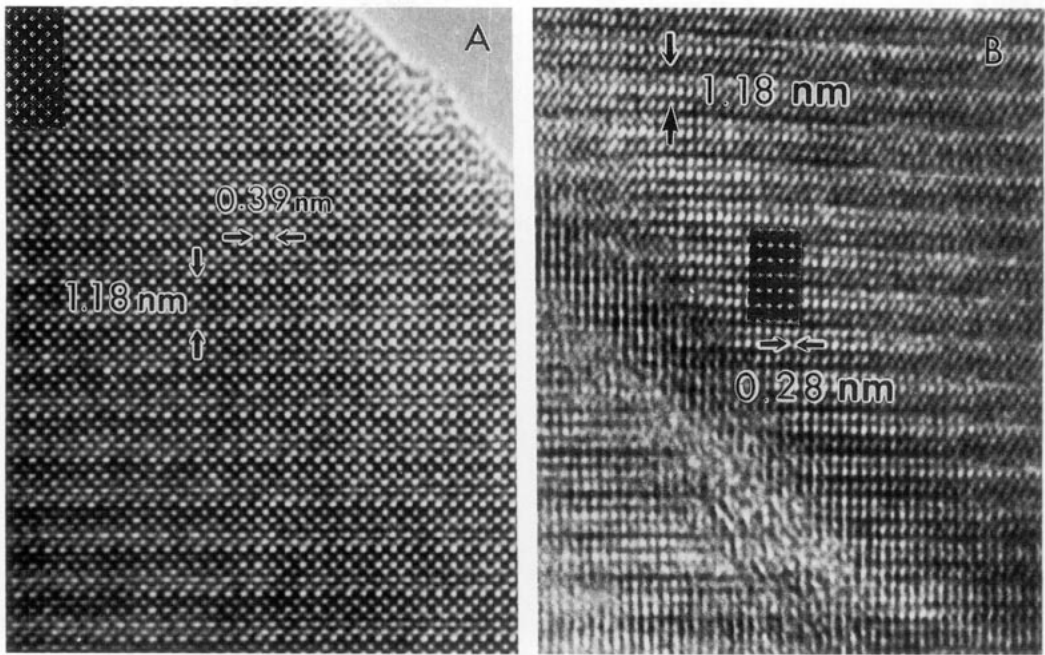


FIG. 3. High resolution images for the  $DyBa_2Fe_3O_8$  material and corresponding calculated images along the (a)  $[010]_c$  and (b)  $[110]_c$  zone axes.

anionic vacancy rows along fixed directions (10, 11). However, the formation of isolated vacancies should lead to fivefold coordination sites.

On the basis of these ideas, it is worth mentioning that the results obtained by Mössbauer spectroscopy on the  $x = 0.33$  material of the  $Ba_xLa_{1-x}FeO_{3-y}$  system (12) show a decrease in the percentage of tetrahedral sites as the  $x$  value increases. In fact, when  $x > 0.5$ , only fivefold and octahedral coordinations are observed for the iron atoms.

Moreover, recent studies by Mössbauer spectroscopy and HREM in the  $Ba_2Fe_2O_5$  material (13, 14) indicated the presence of iron in four-, five-, and sixfold coordination sites.

On the basis of these results, it can be pointed out that when barium is occupying the A positions in the perovskite cationic subcell, iron can adopt also square-pyramidal coordination.

According to this, two possibilities exist for the oxygen distribution:

(a) alternation of two octahedra ( $FeO_6$ ) and one tetrahedron ( $FeO_4$ ) along the  $c$  axis (. . OOTOOT. .) (O = octahedron, T = tetrahedron).

(b) alternation of two square pyramids ( $FeO_5$ ) and one octahedron ( $FeO_6$ ) along the  $c$  axis (. . POPPOP. .) (P = square pyramid).

Both situations are able to produce by themselves a threefold superlattice of the perovskite structure, and they are also compatible with the existence of order between the  $Ln$  and Ba cations.

The first type of distribution corresponds to the  $n = 3$  term of the homologous series  $A_nB_nO_{3n-1}$  (15), and it would give rise to an orthorhombic unit cell of parameters  $a_c \sqrt{2} \times a_c \sqrt{2} \times 3a_c$ . The absence of diffraction maxima doubling the  $(110)_c^*$  reflexion and equivalents (see Fig. 4b in Ref. 16), as well as the image contrast observed in the high resolution micrographs, allow us to propose the second distribution as the most probable to occur. Figure 4 shows the corresponding structure model.

The image contrast has been interpreted

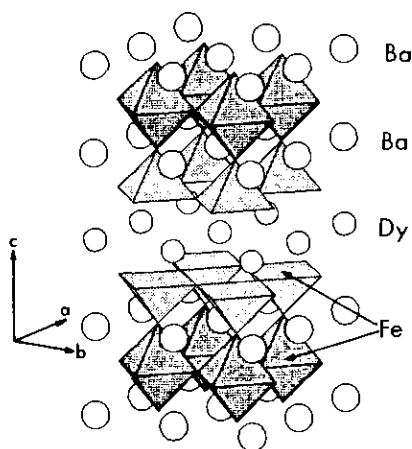


FIG. 4. Structure model proposed for the  $\text{DyBa}_2\text{Fe}_3\text{O}_8$  material.

with the help of a simulation program using the multislice method (17). The image calculations were carried out under the following imaging conditions: sample thickness between 1.7 and 5.5 nm,  $\Delta f = -30$  to  $-70$  nm,  $C_s = 1.0$  nm,  $C_c = 1.7$  nm, beam divergence angle =  $0.8 \times 10^{-3}$  rad, and accelerating voltage = 400 kV.

The structure model used for simulating images was the one represented in Fig. 4 along the  $[010]_c$  and  $[1\bar{1}0]_c$  projections. In a first attempt, both ordered and random distribution in the *A* sublattice were considered. No difference was found in the simulated image contrast, probably due to the closeness of the atomic scattering factors for Ba and Dy/Ho atoms. Because of that, we discuss only the results concerning the ordered structural model.

The agreement is satisfactory for the following conditions:

— $[010]_c$  projection:  $\Delta f = -60$  nm and sample thickness of 2.0 nm.

— $[1\bar{1}0]_c$  projection:  $\Delta f = -60$  nm and sample thickness of 3.8 nm.

Both images are inset in Figs. 3a and b, respectively.

It is worth mentioning that this structural model is the same as one of the two predicted by Galy *et al.* (18) for the  $\text{YBa}_2\text{Cu}_3\text{O}_8$

hypothetical phase. They have described, in a theoretical way, the  $n = 1$ ,  $n = 2$ , and  $n = 3$  terms as derived from a “ $\text{YBa}_2\text{Cu}_3\text{O}_{9-n}$ ” triperovskite through systematic rationalization of the oxygen loss. The  $n = 2$  term would correspond to the  $\text{YBa}_2\text{Cu}_3\text{O}_7$  superconductor (which is a threefold superstructure of the cubic perovskite subcell). The authors proposed two different distributions for the anionic vacancies leading to the  $n = 1$  term ( $\text{YBa}_2\text{Cu}_3\text{O}_8$ ):

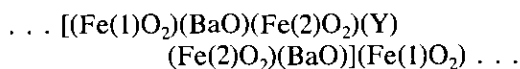
— $\text{YBa}_2\text{Cu}_3\text{O}_8$  (I), where two  $(\text{CuO}_6)$  octahedra layers alternate with a  $[\text{CuO}_4]$  square planar layer along the *c* axis, and

— $\text{YBa}_2\text{Cu}_3\text{O}_8$  (II), constituted by the alternation of two square pyramids  $(\text{CuO}_5)$  and one octahedron  $[\text{CuO}_6]$  along the *c* axis.

The existence of such a term would imply that all the copper is in the III oxidation state. Experimentally, it is difficult to get this situation, and consequently a pure phase showing such an anionic stoichiometry has not yet been obtained. However, it seems easy to achieve it when iron is occupying the *B* positions.

At this point, it is interesting to note that several authors (19, 20) have suggested the existence of domains with  $\text{YBa}_2\text{Cu}_3\text{O}_8$  stoichiometry alternating with others of  $\text{YBa}_2\text{Cu}_3\text{O}_7$  composition. Hervieu *et al.* (19) have proposed form II for the former composition.

Huang *et al.* (7) have solved the structure of the  $\text{YBa}_2\text{Fe}_3\text{O}_8$  material by means of neutron powder diffraction. The structural refinement showed that this compound has tetragonal symmetry, with space group  $P4/mmm$  and lattice parameters  $a = 0.39170$  and  $c = 1.185$  nm. It can be described as formed by a sequence of layers in the following way:



This sequence leads to fivefold pyramidal coordination for Fe(2) and octahedral environment for Fe(1) ions.

From the structural model proposed (Fig.

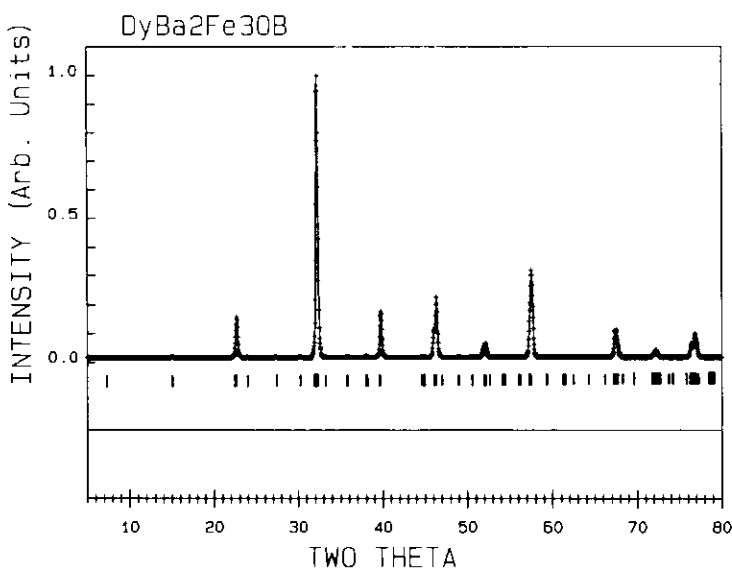


Fig. 5. Calculated X-ray diffraction pattern for  $\text{DyBa}_2\text{Fe}_3\text{O}_8$ .

4) and using the atomic positions obtained by Huang *et al.* for the  $\text{YBa}_2\text{Fe}_3\text{O}_8$  material, we have calculated the X-ray diffraction pattern (21) for  $\text{DyBa}_2\text{Fe}_3\text{O}_8$  (Fig. 5). Discrepancies were not found between the calculated superstructure reflection intensities and those observed by electron and X-ray diffraction. These results seem to reinforce the structural data for the  $\text{Dy}(\text{Ho})\text{Ba}_2\text{Fe}_3\text{O}_8$  materials.

On the other hand, it is worth recalling that the ceramic procedure we have used as synthetic method leads to inhomogeneous products, the 1 : 2 : 3 material being the most abundant. To avoid diffusion problems, several modifications of the ceramic procedure have been utilized; one of them, the so-called liquid mix technique (22), has been developed to synthesize mixed oxides of the perovskite structural type (23). This procedure has been also used by Huang *et al.* (7) to produce a  $\text{YBa}_2\text{Fe}_3\text{O}_8$  single phase. In spite of this, one of the problems concerning the ceramic procedure, the use of long annealing times, could not be avoided by those authors; five firing cycles, each of 300 hr duration, were needed. However, this phase cannot be prepared by the ceramic proce-

dure, a mixture phase being obtained (6). This situation changes as a function of the lanthanide occupying the A sublattice. Moreover, new perovskite-related superstructures, leading to a new homologous series, will be described in a forthcoming paper.

### Acknowledgments

We acknowledge the financial support of C.I.C.Y.T. (Spain) through Research Projects MAT 90-0858-C02-02 and MAT 91-0331, and the MIDAS Program. E.G.G. also thanks the Spanish Ministry of Education for a supporting grant. We are also grateful to Mr. A. García for valuable technical assistance.

### References

1. N. NGUYEN, J. CHOISNET, M. HERVIEU, AND B. RAVEAU, *J. Solid State Chem.* **39**, 120 (1981).
2. C. MICHEL, L. ER-RAKHO, M. HERVIEU, J. PANNETIER, AND B. RAVEAU, *J. Solid State Chem.* **68**, 143 (1988).
3. L. ER-RAKHO, C. MICHEL, P. LACORRE, AND B. RAVEAU, *J. Solid State Chem.* **73**, 531 (1988).
4. C. W. CHU, P. H. HOR, R. L. MENG, L. GAS, Z. I. HUANG, AND I. K. HUANG, *Phys. Rev. Lett.* **58**, 908 (1987).
5. S. GEREMIA, G. NARDIN, R. MOSCA, L. RANDACCIO, AND E. ZANGRANDO, *Solid State Commun.* **72**, 333 (1989).

6. E. GARCÍA-GONZÁLEZ, Ph.D. Thesis, Universidad Complutense, Madrid (April 1992).
7. Q. HUANG, P. KAREN, V. L. KAREN, A. KJEKSHUS, J. W. LYNN, A. D. MIGHELL, N., ROSOV, AND A. SANTORO, *Phys. Rev. B* **45**(17), 9611 (1992).
8. M. PARRAS, E. GARCÍA, J. M. GONZÁLEZ-CALBET, AND M. VALLET-REGÍ, *J. Less-Common Met.* **169**, 25 (1991).
9. J. J. CAPPONI, C. CHAILLOUT, A. W. HEWAT, P. LEJAY, M. MAREZIO, N. NGUYEN, B. RAVEAU, J. L. SOUBEYROUX, J. L. THOLENCE, AND R. TOURNIER, *Europhys. Lett.* **3**, 301 (1987).
10. J. C. GRENIER, L. FOURNES, M. POUCHARD, P. HAGENMULLER, AND S. KOMORNICKI, *Mater. Res. Bull.* **17**, 55 (1982).
11. J. RODRÍGUEZ-CARVAJAL, M. VALLET-REGÍ, AND J. M. GONZÁLEZ-CALBET, *Mater. Res. Bull.* **24**, 423 (1989).
12. J. C. GIBB AND M. MATSUO, *J. Solid State Chem.* **81**, 83 (1989).
13. M. PARRAS, L. FOURNES, J. C. GRENIER, M. POUCHARD, M. VALLET, J. M. GONZÁLEZ-CALBET, AND P. HAGENMULLER, *J. Solid State Chem.* **88**, 261 (1990).
14. X. ZOU, S. HOVMÖLLER, M. PARRAS, J. M. GONZÁLEZ-CALBET, M. VALLET-REGÍ, AND J. C. GRENIER, *Acta Crystallogr. A* **49**, 27 (1993).
15. J. C. GRENIER, M. POUCHARD, AND P. HAGENMULLER, *Struct. Bonding* **47**, 1 (1981).
16. J. M. GONZÁLEZ-CALBET, M. VALLET-REGÍ, M. A. ALARIO-FRANCO, AND J. C. GRENIER, *Mater. Res. Bull.* **18**, 285 (1983).
17. NCEMSS Program, National Center for Electron Microscopy, Materials and Chemical Sciences Division, Lawrence Berkeley Laboratory, University of California, Berkeley, California (1989).
18. J. GALY, R. ENJALBERT, P. MILLET, C. FAULMANN, AND P. CASSOUX, *J. Solid State Chem.* **74**, 356 (1988).
19. M. HERVIEU, B. DOMENGES, C. MICHEL, AND B. RAVEAU, *Europhys. Lett.* **4**, 205 (1987).
20. C. MICHEL, F. DESLANDES, J. PROVOST, P. LEJAY, R. TOURNIER, M. HERVIEU, AND B. RAVEAU, *C.R. Acad. Sci. Ser. 2* **304**, 1059 (1987).
21. H. M. RIETVELD, *J. Appl. Crystallogr.* **2**, 65 (1969).
22. M. PECHINI, U.S. Patent 3 231 328 (1966).
23. M. VALLET-REGÍ, E. GARCÍA-GONZÁLEZ, AND J. M. GONZÁLEZ-CALBET, *J. Chem. Soc. Dalton Trans.*, 775 (1988).